

Heterogeneous nuclear ribonucleoprotein L-like (hnRNPLL) and elongation factor, RNA polymerase II, 2 (ELL2) are regulators of mRNA processing in plasma cells

Micah J. Benson^a, Tarmo Äijö^b, Xing Chang^c, John Gagnon^a, Utz J. Pape^{a,d}, Vivek Anantharaman^e, L. Aravind^e, Juha-Pekka Pursiheimo^f, Shalini Oberdoerffer^g, X. Shirley Liu^d, Riitta Lahesmaa^f, Harri Lähdesmäki^{b,f}, and Anjana Rao^{a,c,h,i,1}

^aDepartment of Pathology, Harvard Medical School and Immune Disease Institute and Program in Cellular and Molecular Medicine, Children's Hospital Boston, Boston, MA 02115; ^bDepartment of Information and Computer Science, Aalto University School of Science, FI-00076 Aalto, Finland; ^cDivision of Signaling and Gene Expression, La Jolla Institute for Allergy and Immunology, La Jolla, CA 92037; ^dDepartment of Biostatistics and Computational Biology, Dana-Farber Cancer Institute and Harvard School of Public Health, Boston, MA 02215; ^eNational Center for Biotechnology Information, National Library of Medicine, National Institutes of Health, Bethesda, MD 20894; ^fMolecular and Systems Immunology and Stem Cell Biology, Turku Centre for Biotechnology, University of Turku and Åbo Akademi University, FI-20520 Turku, Finland; ^gCenter for Cancer Research, Mouse Cancer Genetics Program, National Cancer Institute at Frederick, Frederick, MD, 21702; ^hDepartment of Pharmacology, University of California at San Diego, La Jolla, CA 92037; and ⁱSanford Consortium for Regenerative Medicine, La Jolla, CA 92037

Contributed by Anjana Rao, August 29, 2012 (sent for review July 26, 2012)

B cells and plasma cells possess distinct RNA processing environments that respectively promote the expression of membrane-associated Ig by B cells versus the secretion of Ig by plasma cells. Through a combination of transcriptional profiling and screening using a lentiviral short-hairpin RNA interference library, we show that both the splicing factor hnRNPLL and the transcription elongation factor ELL2 modulate the ratio of secreted versus membrane-encoding *Ighg2b* transcripts in MPC11 plasmacytoma cell lines. hnRNPLL and ELL2 are both highly expressed in primary plasma cells relative to B cells, but hnRNPLL binds *Ighg2b* mRNA transcripts and promotes an increase in levels of the membrane-encoding *Ighg2b* isoform at the expense of the secreted *Ighg2b* isoform, whereas ELL2 counteracts this effect and drives Ig secretion by increasing the frequency of the secreted *Ighg2b* isoform. As in T cells, hnRNPLL also alters the splicing pattern of mRNA encoding the adhesion receptor CD44, promoting exon inclusion, and decreasing the overall level of CD44 expression. Further characterization of ELL2-dependent transcription by RNA-Seq revealed that ~12% of transcripts expressed by plasma cells were differentially processed because of the activities of ELL2, including B-cell maturation antigen BCMA, a receptor with a defined role in plasma cell survival. Taken together, our data identify hnRNPLL and ELL2 as regulators of pre-mRNA processing in plasma cells.

immunoglobulin | mRNA splicing | transcriptional elongation | B cell maturation antigen

One of the earliest examples of a single gene encoding multiple transcripts and protein species was provided by genes encoding the Ig heavy chain (*IgH*) (1–3). The discovery that the *IgH* genes are alternatively processed at their 3' ends explained how they could generate transcripts encoding both membrane-associated and secreted Ig, with B cells primarily expressing the former and plasma cells the latter. The levels of membrane-encoding and secreted *IgH* transcripts are controlled by the mutually exclusive use of a splice site versus a cleavage/polyadenylation [poly(A)] site at the 3' end of the *IgH* pre-mRNA transcript (see diagram in Fig. 1A). In IgG-expressing B cells, the C_H3 exon (or, in IgM-expressing B cells, the C_H4 exon) is spliced to downstream M1 and M2 exons encoding the transmembrane and cytoplasmic domains of membrane Ig (mIg), respectively, with the membrane-associated poly(A) [mbp(A)] site used. In plasma cells, a weak poly(A) sequence [secp(A)] located downstream to the C_H3 exon is included in the final mRNA transcript, with recognition of the secp(A) producing a truncated transcript encoding secreted Ig (sIg) (4, 5). B cells express nearly equivalent levels of *sIgH* and *mIgH* transcripts; upon antigen-driven activation and differentiation into plasma cells, *sIgH* transcripts are overwhelmingly increased in frequency (5, 6). Overall, therefore, the B-cell mRNA processing environment is tilted toward enhanced mRNA splicing at the expense of the

cleavage/polyadenylation reaction (7–9). In contrast, the plasma cell mRNA processing environment is tilted toward enhanced cleavage/polyadenylation processing of pre-mRNA (8, 10). It is likely that these distinct mRNA processing environments reflect the differential presence, in B cells versus plasma cells, of RNA processing factors operating *in trans* on *IgH* pre-mRNA (5, 8).

To identify modulators of pre-mRNA splicing in B cells, we combined transcriptional profiling and a lentiviral shRNA screen to identify RNA-binding proteins that controlled the processing of *IgH* mRNA. We identify the splicing factor hnRNPLL (heterogeneous ribonucleoprotein L-like) and confirm the role of elongation factor RNA polymerase II, 2 (ELL2) in *IgH* pre-mRNA processing (11), and demonstrate that ELL2 is a global regulator of the plasma cell transcriptome.

Results

Microarray Analysis Identifies Differentially Expressed Factors with Predicted mRNA Splicing Function in B Cells and Plasma Cells. Because the distinct *mIgH/sIgH* transcript ratios in B cells and plasma cells are controlled by transcriptional regulators differentially expressed between these two cell types (reviewed in ref. 8), we hypothesized that factors involved in differential processing of *IgH* pre-mRNA in B cells and plasma cells were present in the subset of splicing regulators differentially expressed in these two cell types. To this end, we compared, by microarray, the transcriptional profiles of purified naive mature B cells (B220⁺IgD⁺CD23⁺) and bone marrow resident plasma cells (B220⁺CD138⁺). A list of differentially expressed genes between B cells and plasma cells (twofold change, false-discovery rate 1%) was generated and compared with a list of 307 proteins previously implicated in regulation of pre-mRNA splicing, including members of the serine/arginine rich (SR) and hnRNP families, transcription elongation factors, and SR protein kinases, as well as other proteins containing RNA-recognition motifs.

Within the list of predicted splicing factors, we identified 51 genes (represented by 78 probes), the transcripts of which were differentially expressed between B cells and plasma cells, with 30 genes represented in plasma cells and 21 represented in B cells (Fig. S1A). Among the genes whose transcripts were most highly

Author contributions: M.J.B., T.Ä., S.O., R.L., H.L., and A.R. designed research; M.J.B., T.Ä., X.C., J.G., and J.-P.P. performed research; M.J.B., V.A., and L.A. contributed new reagents/analytic tools; M.J.B., T.Ä., X.C., U.J.P., and X.S.L. analyzed data; and M.J.B. and A.R. wrote the paper.

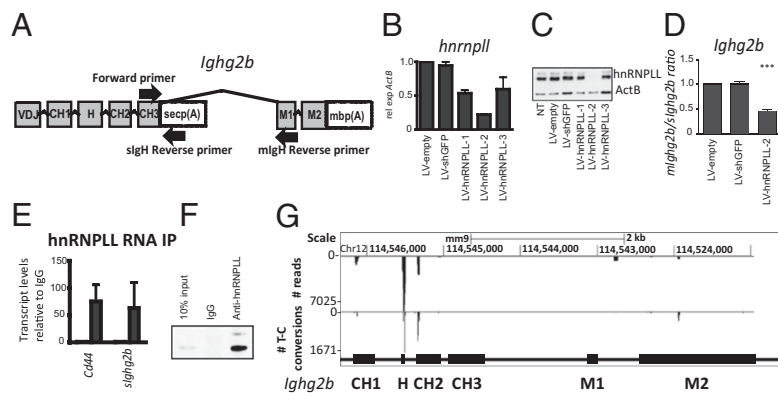
The authors declare no conflict of interest.

Data deposition: The sequences reported in this paper have been deposited in the Gene Expression Omnibus (GEO) database, www.ncbi.nlm.nih.gov/geo (accession nos. GSE39916 and GSE40285).

¹To whom correspondence should be addressed. E-mail: arao@liai.org.

This article contains supporting information online at www.pnas.org/lookup/suppl/doi:10.1073/pnas.1214414109/-DCSupplemental.

Fig. 1. A role for hnRNPLL in *Ighg2b* pre-mRNA exon exclusion. (A) Diagram depicting the intron/exon layout of the *Ighg2b* gene. VDJ indicates a rearranged variable region; CH1-CH3 represent the constant heavy-chain regions 1, 2 and 3; H indicates the hinge exon; M1 and M2 represent the membrane constant exons 1 and 2; secp(A) and mbp(A) represent the secretory and membrane poly(A) sites located in the 3' UTR (dashed boxes), respectively, with the secp(A) residing in a cassette exon that undergoes alternative splicing as indicated. Arrows indicate forward and reverse primers used to quantify *slghg2b* (slgH) and *mlghg2b* (mlgH) isoforms. (B) Levels of *Hnrpll* transcripts in MPC11 cells transduced with lentiviruses targeting *Hnrpll* as assessed by qRT-PCR. Protein levels from the same experiment are shown in C. (D) Levels of *mlghg2b* transcripts levels relative to *slghg2b* in MPC11 cells transduced with the indicated lentiviruses. Results of a Student *t* test are shown as comparisons between the indicated experimental groups, ****P* < 0.001. (E) RNA immunoprecipitation of hnRNPLL from MPC11 lysates, with the levels of associated *CD44* and *Ighg2b* transcripts quantified by qRT-PCR; forward and slgH reverse primers in A were used to quantify *Ighg2b* transcripts. Shown is the fold-enrichment of target transcripts associating with hnRNPLL immunoprecipitates (black bars) in comparison with IgG control (given the arbitrary value of "1"), normalized to 10% input. (F) Immunoblot depicts enrichment of hnRNPLL by anti-hnRNPLL antibodies in comparison with 10% input and control. (G) hnRNPLL binding sites on *Ighg2b* pre-mRNA transcripts as identified by PAR-CLIP. (Upper) Number of PAR-CLIP reads aligning to the *Ighg2b* locus (minus value indicates that the reads were mapped to the reverse strand of DNA). (Lower) Validated reads with T-C transitions indicative of cross-linking. An aligned map of the *Ighg2b* locus is depicted underneath for reference. B, D, and E are combined data from three independent experiments, with error bars expressed as the mean \pm SEM. C and F are representative of two immunoblots.



expressed in plasma cells were *Rbm47*, *Hnrpll* (which encodes the hnRNP family member hnRNPLL), the SR protein *Srsf17b*, and the elongation factor *Ell2*; the genes most highly expressed in B cells included the elongation factor *Ell3* and the SR protein kinase *Srp3* (Fig. S14). Based on these data, we designed a limited shRNA screen to test whether one or more of these factors might modulate IgH alternative splicing.

Expression of hnRNPLL by Plasma Cells. We previously demonstrated that hnRNPLL regulates the alternative splicing of CD45 pre-mRNA in T cells (12). Given the heightened expression of *Hnrpll* transcripts in plasma cells, as indicated by our microarray data as well as public microarray databases (GDS1695), we investigated the expression and functional role of hnRNPLL in plasma cells. Indeed, a mouse plasmacytoma cell line, MPC11, expressed 10-fold higher amounts of *Hnrpll* transcripts compared with the A20 B lymphoma cell line (Fig. S1B). To examine hnRNPLL protein expression, we generated an affinity-purified polyclonal antiserum against a peptide at the N terminus of hnRNPLL (Fig. S24). Two hnRNPLL bands (65 and 80 kDa) were observed in immunoblots of MPC11 cell lysates with the anti-hnRNPLL antiserum (Fig. S1C and E): the more abundant 65-kDa isoform corresponds to the predicted molecular weight of hnRNPLL based on published protein sequences (National Center for Biotechnology Information Ref Seq NP_659051.3).

We also examined *Hnrpll* mRNA and protein expression by in vitro-activated murine CD4 T cells and B cells. Naive CD4 T cells express *Hnrpll* mRNA, with transcript levels doubling upon 72 h of activation with anti-CD3/CD28 (Fig. S1D); there was little change in hnRNPLL protein levels (Fig. S1E). Even though we could not detect expression of *Hnrpll* by naive B cells, B cells activated for 72 h by various conditions expressed detectable levels of *Hnrpll* mRNA transcripts, although at greatly diminished levels compared with naive or activated T cells (Fig. S1D). The low expression of hnRNPLL by activated B cells was also evident at the protein level (Fig. S1E).

Sorted B220⁺CD138⁺ plasma cells exhibited an ~20-fold increase in *Hnrpll* transcript levels compared with B220⁺ B cells (Fig. S1F), and observed heightened expression of hnRNPLL by intracellular staining in the plasma cell population compared with total B220⁺ B cells (Fig. S1G). We also examined the expression pattern of hnRNPLL in CD4⁺ T cells, with CD4⁺CD44⁺ cells showing greater hnRNPLL expression than CD4⁺CD44⁻ T cells (Fig. S2B), consistent with higher hnRNPLL expression by human activated/memory T cells (12). Antibody

specificity was verified by decreased hnRNPLL staining upon shRNA-mediated knockdown of hnRNPLL in MPC11 cell lines (Fig. S2C). Taken together, these data confirm that hnRNPLL is expressed at the protein level in plasma cells.

hnRNPLL Directly Associates with and Influences the Splicing Fate of IgH and CD44 Pre-mRNA Transcripts. The heightened expression of hnRNPLL by plasma cells in comparison with B cells, and the opposing abilities of these respective cell types to process IgH mRNA, prompted us to examine the potential role of hnRNPLL in IgH pre-mRNA processing. Using the MPC11 plasmacytoma cell line, we developed a quantitative RT-PCR (qRT-PCR)-based assay that quantifies the relative amounts of membrane associated (*mlghg2b*) and secreted (*slghg2b*) *Ighg2b* transcripts using a common primer situated on the C_H3 exon of *Ighg2b* (forward primer) and reverse primers situated either on the cassette exon containing the secp(A) site (slgH reverse primer) or the *Ighg2b* M1 exon (mlgH reverse primer) (Fig. 1A). Based on this assay, we estimated the basal *slghg2b*:*mlghg2b* ratio to be 45:1 in MPC11 cells, a ratio consistent with previous data on plasmacytoma cell lines (4). To deplete hnRNPLL protein in MPC11 cells, we transduced MPC11 cells with pLKO.1 lentivirus encoding short hairpins (shRNAs) that target *Hnrpll* transcripts. After eliminating untransduced cells by selection with puromycin, we achieved ~80% knockdown of *Hnrpll* mRNA transcripts and almost complete depletion of hnRNPLL protein in cells transduced with LV-hnRNPLL-shRNA#2, compared with cells transduced with empty pLKO.1 vector or a vector encoding a hairpin specific to GFP (Fig. 1B and C). hnRNPLL depletion in MPC11 cells was associated with a twofold reduction in the ratio of *mlghg2b* to *slghg2b* mRNA (Fig. 1D). These results suggested that depletion of hnRNPLL in MPC11 cells increased utilization of the secp(A)-containing cassette exon.

We next asked whether hnRNPLL directly associated with *Ighg2b* mRNA in MPC11 cells. We used RNA-immunoprecipitation—that is, hnRNPLL immunoprecipitation followed by qRT-PCR—to quantify *Ighg2b* mRNA transcripts bound to hnRNPLL. We additionally tested for the presence of *Cd44* mRNA transcripts, a known target of hnRNPLL in T cells (12), in hnRNPLL immunoprecipitates. Compared with immunoprecipitates prepared with control IgG, hnRNPLL immunoprecipitates showed strong enrichment for both *Cd44* and *Ighg2b* mRNA transcripts (Fig. 1E and F). To precisely identify the hnRNPLL binding sites within *Ighg2b* transcripts, we performed photoactivatable-ribonucleoside-enhanced cross-linking and immunoprecipitation (PAR-CLIP) (13) (Fig. 1G). A feature of PAR-CLIP is that cross-linked

RNAs can be distinguished from contaminating or spurious non-cross-linked RNAs by a discernible increase in the frequency of T > C transitions at the sites of RNA-protein cross-linking when using 4-thiouridine, with this feature used to distinguish true RNA partners for a given protein, and moreover experimentally pinpoint sites in the vicinity of RNA-protein cross-links (13). Based on the presence of T > C transitions, major peaks of hnRNPLL binding were identified within the H and C_H2 exons of *Ighg2b*, with peaks observed in the C_H1, H, C_H2, and M2 exons (Fig. 1G). Taken together, these data demonstrate that hnRNPLL modulates *Ighg2b* pre-mRNA processing and facilitates secp(A) exon exclusion through direct association with *Ighg2b* pre-mRNA.

Consistent with our previous findings that hnRNPLL promotes *Cd44* exon exclusion in T cells (12), we observed that depletion of hnRNPLL promoted exon retention in MPC11 cells (Fig. 2B), as assessed by RT-PCR analysis using primers book-ending the *Cd44* cassette exons (Fig. 2A). In addition, increased *Cd44* transcript and CD44 protein levels were observed upon hnRNPLL depletion (Fig. 2C and D). Through analysis of reads with T > C transitions that aligned to the *Cd44* locus after hnRNPLL PAR-CLIP, we identified multiple hnRNPLL binding sites within the intervening introns of the *Cd44* cassette exons (Fig. 2E), as well as within exon 1. These results indicate that hnRNPLL directly associates with *Cd44* pre-mRNA transcripts and modulates both the alternative splicing of *Cd44* pre-mRNA and the expression levels of CD44 protein.

Lentiviral shRNA Screen Confirms ELL2 as a Regulator of Ig Processing in Plasma Cells. The results described in Fig. 1 indicated that hnRNPLL drives expression of mIg at the expense of sIg, thus unexpectedly countering rather than promoting Ig secretion by plasma cells. This finding implied that other *trans* factors expressed in plasma cells dominantly counteract this function of hnRNPLL and drive production of the sIgH isoform. To identify

these factors, we performed a lentiviral shRNA screen in the IgG2b-secreting MPC11 plasmacytoma cell line and the IgG2a-expressing A20 B lymphoma cell line, focusing on the candidate targets most strikingly differentially expressed in either plasma cells (24 of 30 targets were pursued) or B cells (12 of 21 targets were pursued). The levels of mIgH and sIgH in MPC11 and A20 cells were quantified using the qRT-PCR method presented in Fig. 1; combined primary and secondary screening data are shown in Fig. 3A and B. Three hairpins targeting the ELL2 protein increased the ratio of *mIghg2b* to *sIghg2b* in MPC11 cells (Fig. 3A). No significant hits were observed in the B-cell screen (Fig. 3B).

We examined the expression patterns of candidates in A20 and MPC11 cell lines. Consistent with the expression patterns observed in primary cells (Fig. S1A), *Ell2*, *Rbm47*, and *Gdap2* transcripts were enriched in plasma cells, and *Zcchc7*, *Ell3*, and *Srpk3* transcripts were enriched in B cells (Fig. S3). ELL2 was previously identified as a protein capable of driving sIgH accumulation in plasma cells (11). By qRT-PCR, we observed that several activation conditions (72 h) induced *Ell2* transcript accumulation in B cells; in contrast, CD4 T cells showed no changes in transcript levels upon activation with anti-CD3 and anti-CD28 (Fig. 3C). Moreover, plasma cells sorted *ex vivo* exhibited an approximately fivefold increase in mRNA transcript levels compared with naive mature B cells (Fig. 3D). To confirm the role of ELL2 in IgH pre-mRNA processing, we depleted *Ell2* transcripts in MPC11 cells. When the two best hairpins, ELL2-1C7 and ELL2-1C11, were transduced into MPC11 cells, in each case depleting *Ell2* transcripts by at least 80% (Fig. 3E), a fourfold increase in levels of *mIghg2b* mRNA relative to *sIghg2b* was observed (Fig. 3F). This increase of *mIghg2b* relative to *sIghg2b* was the result of a twofold increase in *mIghg2b* levels and a twofold decrease in total *sIghg2b* levels (Fig. 3G). Finally, the reduction in *sIghg2b* transcript levels resulting from ELL2 knockdown resulted in a concomitant reduction in the amount of Ig secreted by the MPC11 cell line (Fig. 3H). Taken together, these data validate ELL2 as modulating IgH mRNA processing and implicate ELL2 as necessary for optimal Ig production and secretion by plasma cells.

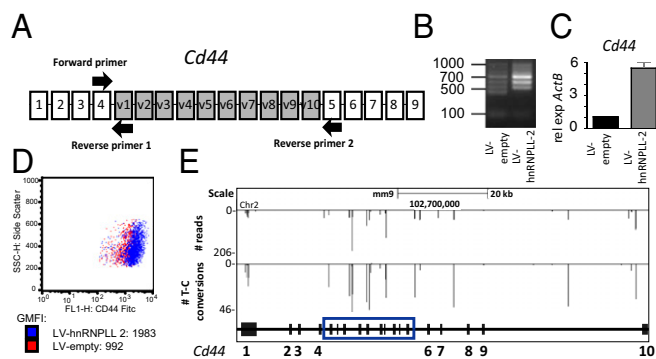
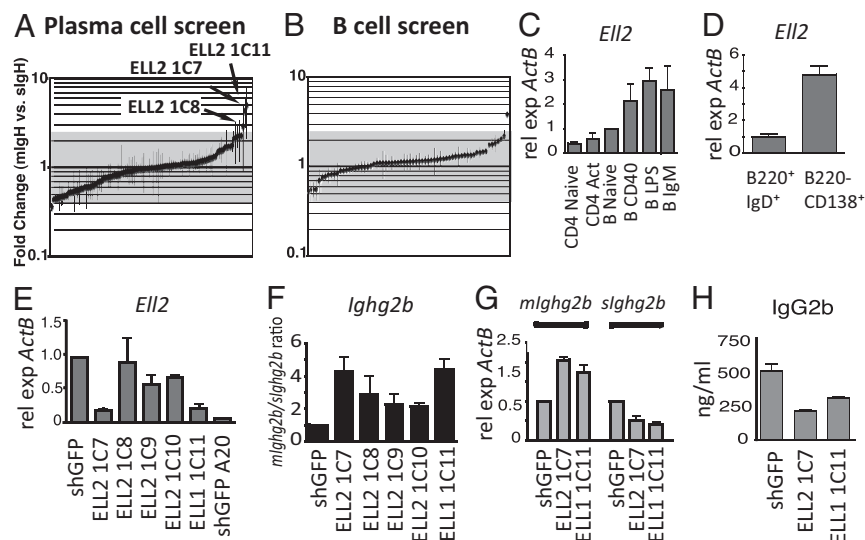


Fig. 2. Modulation of CD44 expression by hnRNPLL in plasma cells (PCs). (A) Diagram depicting the intron/exon layout of the *Cd44* gene. Constitutive exons are shown in white, variable cassette exons are shaded and are denoted by "v1-10." Forward and reverse arrows indicate locations of the primers used for assays performed in B and C. (B) hnRNPLL controls the alternative processing of *Cd44* mRNA transcripts in PCs. RT-PCR assay using forward primer 1 and reverse primer 2 on RNA from MPC11 cells transduced with empty or hnRNPLL-knockdown lentivirus. hnRNPLL depletion results in increased exon retention. (C) hnRNPLL depletion increases the expression of total *Cd44* transcripts. qRT-PCR analysis measuring *Cd44* transcripts using forward primer 1 and reverse primer 1 in A on transduced MPC11 cells, as depicted. (D) hnRNPLL depletion leads to increased surface expression of CD44. Expression of CD44 by MPC11 cells transduced with the indicated lentivirus as measured by FACS. Legend on bottom indicates the geometric mean fluorescent intensity of CD44 for the indicated cell type. Data representative of *n* = 2 experiments. (E) PAR-CLIP was used to identify hnRNPLL binding sites on *Cd44* pre-mRNA transcripts. (Upper) Number of PAR-CLIP reads on the *Cd44* locus (minus value indicates that the reads were mapped to the reverse strand of DNA). (Lower) Validated reads with T-C transitions indicative of cross-linking. An aligned map of the *Cd44* locus is depicted underneath for reference, with constitutive exons labeled and cassette exons v1-10 present in a blue box.

Global Identification of ELL2-Dependent mRNA Processing Events. To test whether ELL2 regulates a broad program of pre-mRNA processing in plasma cells, we performed RNA-sequencing on MPC11 cell lines transduced with either pLKO.1-shGFP (hereafter referred to as shGFP) or pLKO.1-shELL2-1C7 (referred to as shELL2) lentiviruses. For the shGFP and shGFP samples, 203 and 243 million reads were generated, of which 66% and 70%, respectively, mapped to the genome. Of reads mapping to the genome, 40% mapped to exons for the shGFP samples and 39% mapped to exons for the shELL2 samples, with 3 million and 3.9 million reads aligning to splice junctions or alternative exons for the shGFP and shELL2 samples, respectively. Manual inspection of reads aligning to *Ell2* exons confirmed successful depletion of *Ell2* transcripts in the shELL2 compared with the shGFP MPC11 cell line (Fig. S4A), in contrast to similar frequencies of reads aligning to the *Gapdh* and *Actb* gene bodies (Fig. S4B and C). Negative binomial-based differential expression analysis (14) pointed to a 10-fold decrease in expression of *Ell2* transcripts (corrected *P* value of 1.23E-09). Expression levels of *Ighg2b* transcripts were similarly analyzed using both a gene- and an exon-centric approach. Upon ELL2 depletion, reads aligning to the entire gene body of *Ighg2b* were reduced twofold (*P* = 0.013) (Fig. S4D). When the expression levels of each exon were compared between the two treatment groups, we observed a consistent twofold loss of expression of the C_H1, C_H2, and C_H3 exons (Table S1). Conversely, reads aligning to the M1 and M2 exons in the shELL2 samples were increased, although not statistically significantly, with fold-change increases of 1.52 (*P* = 0.17) and 2.15 (*P* = 0.46), respectively (Table S1). This twofold decrease in *sIghg2b* transcripts and twofold increase in *mIghg2b* transcripts observed upon ELL2 depletion is in agreement with our qRT-PCR data (Fig. 3G).

The RNA-Seq data were used to assess how ELL2 controls the expression patterns of alternative transcript isoforms at the

Fig. 3. A lentiviral screen confirms ELL2 as a regulator of IgH2b mRNA processing in plasma cells. To identify factors involved in IgH mRNA processing, MPC11 or A20 cells were transduced with pLKO.1 lentiviruses targeting potential splicing factors, selected, and expanded. (A and B) Each datapoint represents the mlgH/slgH ratio of a single pLKO.1 splicing factor-targeting hairpin relative to pLKO.1-shGFP controls of MPC11 or A20 cells, with error bars indicating SD. Gray areas indicate 2 SDs from the mean. Sample labels in A indicate hits. (C) *Ell2* transcript levels of naive and 72 h in vitro-activated B and T cells were quantified by qRT-PCR. (D) qRT-PCR expression of *Ell2* transcripts in sorted B220⁺CD138⁺ plasma cells and B220⁺IgD⁺ B cells. (E) MPC11 cells were transduced with lentiviruses targeting *Ell2* transcripts, with selected cells analyzed for *Ell2* mRNA transcript levels by qRT-PCR. (F) Quantification of *mlghg2b* mRNA transcript levels relative to *slghg2b* in MPC11 cells transduced and selected with the indicated lentiviruses. (G) Same experiment as in F, except quantification of *mlghg2b* and *slghg2b* mRNA relative to *Actb* is depicted. (H) MPC11 cells transduced with the indicated lentivirus were cultured at equivalent cell densities for 4 h, with supernatants harvested and analyzed to quantify secreted IgG2b. C–G are pooled data from three independent experiments and H is representative of two independent experiments. Error bars are expressed as the mean \pm SEM.



transcriptome level. We used the mixture-of-isoforms (MISO) model to estimate expression levels of different mRNA isoforms (15) by quantifying the presence of alternatively spliced exons and 3' poly(A) sites residing on UTRs, using significance thresholds of Bayes Factor > 10 and RPKM > 1 (reads per kilobase per million reads). This methodology allowed us to: (i) identify targets for which ELL2 modulates the following pre-mRNA processing event subclasses: tandem 3' UTRs, mutually exclusive exons, skipped exons, alternative 3' and 5' splice sites, retained introns, and alternative first and last exons (depicted in Fig. 4A); and (ii) query whether ELL2 depletion led to preferential inclusion or exclusion of alternative exons and UTRs. We calculated the "percent spliced in (Ψ)" value for cassette exons and UTRs in the shGFP and shELL2 samples (15). We observed significant changes in mRNA processing in each type of event subclass analyzed, with exons and UTRs preferentially included as well as excluded upon ELL2 depletion (Fig. 4B). In total, of 10,376 transcripts annotated, 1,248 transcripts (12% of total) were differentially processed upon ELL2 depletion, indicating a broad role for ELL2 in regulating mRNA processing events in plasma cells. Many genes were found to undergo multiple types of differential splicing events ELL2 depletion (Dataset S1) and, in addition, to undergo two or more differential splicing event classes. Taken together, these results indicate widespread changes in mRNA processing occurring as a result of ELL2 depletion in plasma cells.

We determined the directionality of exons and UTR exclusion versus inclusion in transcripts whose alternative splicing and tandem UTR use were influenced by ELL2. To quantify this determination, we calculated $\Delta\Psi$, the difference in Ψ values for each type of splicing event between the shGFP and shELL2 samples. A $\Delta\Psi > 0$ indicates a preference for cassette exon or UTR inclusion, whereas a $\Delta\Psi < 0$ indicates a preference for cassette exon or promoter distal UTR exclusion upon ELL2 depletion. For all splicing event subclasses, we observed a nearly equal frequency of events where exons were included versus excluded (Fig. 4B). Despite the high frequency of differentially occurring mRNA processing events resulting from ELL2 depletion, a statistically significant directional bias was not observed for any event subclass as the mean of $\Delta\Psi$ did not significantly deviate from 0 (Fig. 4C). Fig. 4C also shows that the $\Delta\Psi$ values for alternative last exon events modulated by ELL2 deviated significantly from those observed for all other subclasses of pre-mRNA processing events (significance determined by

ANOVA with Bonferroni posttest, $P < 0.001$), indicating that splicing events involving the last exon are significantly less influenced by ELL2 depletion compared with other subclasses of splicing events. In summary, we conclude that despite the high frequency of transcripts whose processing is modulated by ELL2 and the clear effect of ELL2 depletion on secp(A) exon exclusion and tandem UTR use at the *Igh* locus, we do not observe an overt directional bias imposed on specific subclasses of pre-mRNA processing events at the transcriptome level.

We additionally performed GeneTrail Advanced Gene Set Enrichment Analysis (GSEA) to examine whether transcripts modified by ELL2 were enriched for particular functional categories. A number of subcategories were significantly enriched (Table S2). The top category was the spliceosome, with many core and regulatory components (including members of the SR and hnRNP families) as well as components of the transcription/export (TREX) complex found affected by ELL2 depletion. Transcripts encoding proteins involved in the RNA degradation pathway were also strongly regulated by ELL2, including components of the deadenylase complex and the exosome. Many components of the ribosome were also targeted by ELL2. Finally, ELL2 also modified protein-processing pathways as components of the protein export pathway, including sec proteins, and a number of proteins involved in ubiquitin-mediated proteolysis were affected. We conclude from these results that that ELL2 preferentially processes transcripts encoding protein products involved in RNA and protein processing.

ELL2 Is Required for the Expression of B Cell Maturation Protein by Plasma Cells. We performed differential gene expression (DESeq) analysis to identify changes in overall gene expression levels between shGFP and shELL2 samples. Upon ELL2 depletion, the transcript levels of *Tsc22d1*, a TGF- β -induced gene, were significantly increased, and those of *Tnfrsf17* (encoding the B-cell maturation protein, BCMA, a receptor with a known role in plasma cell function) and *Ccnb2* (encoding cyclin B2) were significantly suppressed (Table S1). Manual analysis of reads aligning to the *Tnfrsf17* locus found that reads corresponding to all three exons were indeed lost upon ELL2 depletion (Fig. 5A). We validated this finding, as well as the differential transcript levels of *Tsc22d1* and *Ccnb2*, by qRT-PCR (Fig. 5B). Notably, the expression levels of *Tnfrsf17* transcripts were reduced over 20-fold. At the protein level, we were unable to detect BCMA on the surface of MPC11 cells depleted for ELL2 by transduction

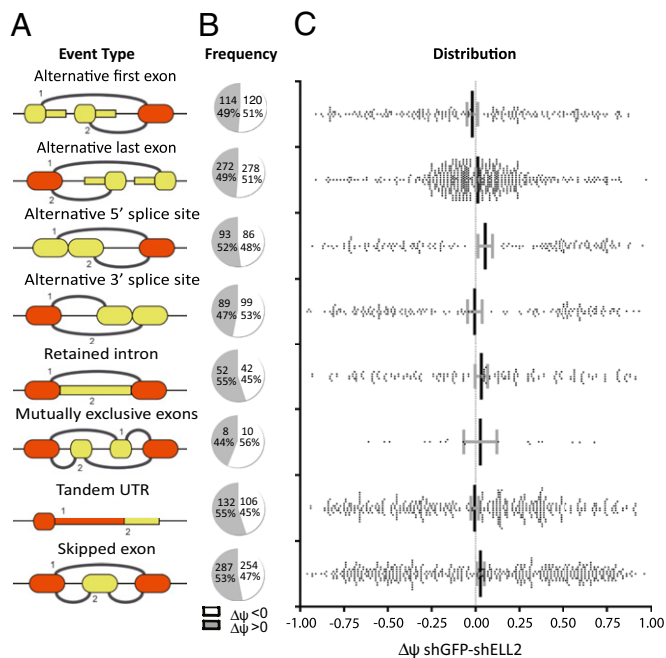


Fig. 4. Global identification of ELL2-dependent mRNA processing events. Alternative mRNA processing events mediated by ELL2 were identified in pLKO.1-shGFP and pLKO.1-shELL2-transduced MPC11 cell lines by performing RNA-Seq and analyzing using the MISO model. (A) The types of mRNA processing events analyzed are depicted, with the alternative exons or UTRs of the pre-mRNA shown in yellow and the constant regions shown in orange. (B) For each type of mRNA processing event, pie charts depict the number of target genes modulated that have either reduced (yellow) or increased (orange) alternative exon or UTR use upon knockdown of ELL2 as measured by the change in percent spliced in ($\Delta\Psi$). (C) The distribution of $\Delta\Psi$ values between control and ELL2-knockdown samples for each type of alternative processing event with each modulated target gene depicted as a dot. The mean \pm SEM of all $\Delta\Psi$ values for each type of alternative processing event shown. No significance was found between the mean of $\Delta\Psi$ for each alternative processing event and 0 by a Wilcoxon rank sum test.

with shELL2, although shGFP-transduced MPC11 cells expressed detectable levels of BCMA, as shown by flow cytometry (Fig. 5C). These data demonstrate an essential role for ELL2 in driving the expression of BCMA in plasma cells.

The model that emerges from these collective data are a plasma cell gene regulatory network that incorporates ELL2 and hnRNPLL as pre-mRNA modulating factors that function downstream of the transcriptional regulators driving the plasma cell state, with Blimp1 controlling hnRNPLL expression and IRF4 controlling ELL2 expression (16, 17). These factors, hnRNPLL and ELL2, contribute to the plasma cell state by controlling the pre-mRNA processing of network of transcripts, including those encoding IgH2b and BCMA (Fig. 5D).

Discussion

A growing body of evidence supports the concept that cellular growth, survival, differentiation, and apoptosis are regulated by factors controlling pre-mRNA processing. In many cases, a single factor controls the differential processing of an entire network of gene products and can function as a regulatory switch both at the cellular and organism level (18, 19). Our presented study identifies and characterizes hnRNPLL and ELL2 as expressed in plasma cells, with both proteins regulating the processing of multiple mRNA targets and, by regulation of IgH, CD44, and BCMA plasma cell function.

Through an shRNA screen in T cells, we identified hnRNPLL as a major regulator of CD45 pre-mRNA processing (12). It is apparent that the influence of hnRNPLL on T-cell function goes

beyond its ability to facilitate exon exclusion in CD45 pre-mRNA transcripts (12, 20), as indicated by the effect on processing of diverse target mRNAs in activated T cells (12, 20), and because breeding a mouse strain harboring a hnRNPLL V136D mutation onto a CD45-deficient background did not mitigate the functional impact of the hnRNPLL V136D mutation on in vivo T-cell survival and homeostasis (21). In plasma cells as in T cells (12), hnRNPLL regulates the alternative splicing of CD44 pre-mRNA, indicating an overlap of targets between these two cell types. In plasma cells, we show here that hnRNPLL directly associates with IgH mRNA, and that ablation of hnRNPLL leads to increased recognition of the weak scsp(A) site and heightened accumulation of the sIgH isoform. The role hnRNPLL plays in plasma cell function in vivo remains to be defined.

Using an approach similar to the one we employed to identify hnRNPLL as a regulator of CD45 pre-mRNA splicing (12), we used a candidate shRNA-lentiviral screen on B-cell and plasma cells lines to screen for factors modulating IgH pre-mRNA processing. Our data confirm previous work by Milcarek and colleagues (11), who demonstrated that the transcription elongation factor ELL2 was highly expressed and able to enhance IgH exon skipping and polyadenylation in plasma cells.

To analyze further how ELL2 functions in plasma cells and define its influence on the overall plasma cell transcriptome, we performed RNA-Seq on a plasmacytoma cell line in which ELL2 expression had been silenced by shRNA. It was clear from our RNA-Seq analysis that ELL2 modified the processing of a broad number of transcripts. Notably, ELL2 depletion did not particularly bias the plasma cell pre-mRNA cleavage/ polyadenylation/ splicing environment toward increased exon skipping or promoter-proximal tandem UTR use. The directional bias observed at the IgH gene, and the absence of this bias at the broader transcriptome level, may reflect an exquisite sensitivity of IgH pre-mRNA to modest changes in the splicing environment, resulting from the mutually exclusive nature of the cleavage/ polyadenylation and splicing reaction and the weak scsp(A) and 5' splice sites (8). For example, separation of the tandem poly(A) sites of the IgH gene from the competing splice reaction and introduction of these IgH minigenes into B-cell and plasma cell lines resulted in an increase in sec(A) site use by only twofold in plasma cells compared with B cells (8, 22–24). Similarly, separation of the IgH gene splicing reaction from the cleavage/ polyadenylation reaction by use of minigenes, and subsequent introduction of these constructs into B-cell and plasma cell lines resulted in greater rates of splicing by B-cell lines (7). However, the researchers went to great lengths to generate a minigene sensitive enough to detect this difference: to observe and amplify the difference in splicing environments, a weakened 5' splice site had to be used (7). Furthermore, previous attempts to identify splicing environment differences between B cells and plasma cells yielded inconclusive results, indicating that the assays that were used were not sensitive enough to detect these differences (24, 25). Given the sensitivity of the IgH gene to changes in cleavage/ polyadenylation and splicing environment, it is not surprising that we did not observe any overt directional bias in splicing or tandem UTR use at the transcriptome level in our RNA-Seq results.

Our finding that ELL2 is required for the expression of BCMA directly links ELL2 to in vivo plasma cell function. BCMA (encoded by *Tnfrsf17*) is selectively expressed by plasma cells within the B-cell lineage, and upon engagement with its ligands BAFF and APRIL in the context of a pro-survival environmental niche, BCMA provides plasma cells with critical survival signals enabling their long-term persistence in the host (26, 27). In the absence of BCMA expression, the establishment of long-lived plasma cells in the bone marrow is defective, leading to impaired long-term humoral memory (27). How ELL2 is so dramatically required for the expression of BCMA, and whether this effect is direct, remains to be mechanistically elucidated. The ablation of BCMA expression upon depletion of ELL2 in cell lines hints at an essential role for ELL2 in plasma cell survival in an in vivo

